PURA and GLUT1: Sweet partners for brain health

Rocío B. Colombo[1,2], Clarisa Maxit[3], Diego Martinelli[4], Mel Anderson[5], Diego Masone[1,6], Lía Mayorga[1,7]

1-Instituto de Histología y Embriología de Mendoza (IHEM), Consejo Nacional de Investigaciones Científicas y Técnicas (CONICET), Universidad Nacional de Cuyo (UNCuyo), Mendoza, Argentina.
2- Facultad De Química, Bioquímica y Farmacia, Universidad Nacional De San Luis San Luis, Argentina.
3- Servicio de Neurología infantil, Hospital Italiano de Buenos Aires, Buenos Aires, Argentina.
4- Division of Metabolism, Bambino Gesù Children's Hospital, Rome, Italy.
5- PURA Foundation Australia , Plenty Victoria, Australia.
6-Facultad de Ingeniería, Universidad Nacional de Cuyo (UNCuyo).
7- Instituto de Neurología Infantojuvenil (Neuroinfan), Mendoza, Argentina.

ABSTRACT

PURA, also known as Pur-alpha, is an evolutionarily conserved DNA/RNA-binding protein crucial for various cellular processes, including DNA replication, transcriptional regulation, and translational control. Comprising three PUR domains, it engages with nucleic acids and has a role in protein-protein interactions. The manifestation of PURA syndrome, arising from mutations in the PURA gene, presents neurologically with developmental delay, hypotonia, and seizures. In our prior work from 2018, we highlighted the unique case of a PURA patient displaying hypoglycorrhachia, suggesting a potential association with GLUT1 dysfunction in this syndrome.

In this current study, we expand the patient cohort with PURA mutations exhibiting hypoglycorrhachia and aim to unravel the molecular basis of this phenomenon. We established an in vitro model in HeLa cells to modulate PURA expression and investigated GLUT1 function and expression. Our findings indicate that PURA levels directly impact glucose uptake through the functioning of GLUT1, without influencing significantly GLUT1 expression. Moreover, our study reveals convincing evidence for a physical interaction between PURA and GLUT1, demonstrated by colocalization and co-immunoprecipitation of both proteins. Computational analyses, employing molecular dynamics, further corroborates these findings, demonstrating that PURA:GLUT1 interactions are plausible, and that the stability of the complex is altered when PURA is truncated and/or mutated.

In conclusion, our results suggest that PURA plays a pivotal role in driving the function of GLUT1 for glucose uptake, potentially forming a regulatory complex. Additional investigations are warranted to elucidate the precise mechanisms governing this complex and its significance in ensuring proper GLUT1 function.

INTRODUCTION

The protein PURA, also known as Pur-alpha, is a highly conserved single-stranded DNA/RNA binding protein with intricate involvement in various cellular processes, including DNA replication, RNA processing, transcriptional and translational regulation[1]. Since its initial

characterization in 1992 in HeLa cells [2], extensive research has revealed its multifaceted roles in modulating the functions of numerous molecules across different cellular compartments.

As a member of the PUR family, PURA comprises three highly conserved sequence-specific repeats known as PUR domains I, II, and III, which play a fundamental role in the protein's primary functions[3]. Each PUR amino acid repeat is characterized by a structural configuration featuring a β-sheet domain and an α-helical domain organized in a "whirly fold" arrangement. In this structure, the convex β-sheets provide a surface for interactions with nucleic acids, while the remaining helical portions are actively engaged in protein-protein interactions[4]. Regarding protein-protein interactions, specifically, the PUR I and II motifs are suggested to establish intramolecular peptide-peptide bonds with each other. In contrast, the PUR III domain assumes the responsibility of facilitating homo-heterodimerization with another PUR protein or interacting with other proteins[3,5].

Although initially described as primarily localized in the nucleus, PURA has demonstrated pivotal functions spanning various cellular domains. Within the nucleus, PURA binds to distinct DNA promoter regions of genes, such as MBP[6], CD43[7–10], and GATA2[11]. In addition, it can collaborate synergistically with transcription factors like E2F1[12,13]. Furthermore, it exhibits binding affinity towards circular RNAs [14] and non-coding RNAs[15], exerting notable influences on gene transcription. Additionally, PURA plays a significant role in DNA repair processes[16,17].

In the cytoplasm, PURA's capabilities extend to mRNA binding, promoting site-specific translation and participating in the formation of RNA binding protein (RBP) granules, including but not limited to BCL1, MAP2, Stau1, Myo5A, and FMR1 [18,19]. Direct protein-protein interactions have been observed with KIF1[20] and other members of the PUR family[4,21].

Notably, PURA emerges as a crucial player in disease scenarios, particularly in conditions involving CGG repeat-expanded FMR1 (Fragile-X syndrome) [22,23] and G_4C_2 repeat expansions in C9orf72, contributing to Amyotrophic Lateral Sclerosis and Frontotemporal degeneration (ALS/FTD) [24,25]. Here, it binds to anomalous RNAs, serving a protective role against neurotoxicity.

The advent of next-generation sequencing and high-throughput genetic technologies in clinical practice has led to increased identification of patients with PURA syndrome[26–35]. PURA syndrome, a rare genetic condition resulting from mutations in the PURA gene, manifests as a spectrum of clinical features, mainly neurological, including developmental delay, hypotonia, breathing difficulties, pituitary dysfunction, and seizures[26–35]. Evidently, PURA's indispensable role in neuronal development and function is underscored by these clinical findings in patients and by evidence gained from two knock-out mouse models[36,37], which exhibited severe tremors, seizures, movement disorders associated with alterations in brain size, cell distribution and premature death. Intriguingly, one of the knock-out models was pointed out to be able to extend their short lifespan with periodical glucose injections[36]. Furthermore, human patients with PURA syndrome, have been described to manifest with hypoglycemia[30] introducing a possible link between PURA and glucose metabolism.

The transportation of glucose across the blood-brain barrier predominantly relies on the glucose transporter 1 (GLUT1 or SLC2A1), highly expressed in endothelial cells, astrocytes and red blood cells[[38]. Mutations in GLUT1 give rise to GLUT1 deficiency syndrome, characterized by seizures, developmental delay, and movement disorders, accompanied by the disorder´s hallmark: hypoglycorrhachia (low cerebrospinal fluid glucose levels) [39,40]. Notably, PURA syndrome and GLUT1 deficiency share numerous neurological clinical features, but hypoglycorrhachia was first reported by us in 2018 in a PURA syndrome patient[35]. This discovery suggested a potential connection between PURA and GLUT1. In this current study, we expand the cohort of patients suffering from PURA deficiency, who also displayed hypoglycorrhachia. This intriguing observation served as the cornerstone of our research, laying the foundation for our findings that establish a direct link between PURA and GLUT1.

METHODS

Patient data: PURA deficiency patients´ data were gathered from medical records from the care-giving centers and physicians.

Cell culture: Human HeLa (CCL-2) cells were purchased from ATCC, The Global Bioresource Center and grown in DMEM high-glucose (Gibco®, cat#11995065) in 5% CO_2 supplemented with 10% fetal bovine serum (Gibco®, cat#16000044), 100U/ml Penicilin+ Streptomicine (Gibco®, cat#15140122). Passages 20-38 were used for experiments. The six experimental conditions used for experiments were created as follows:

1_ Control. Generation of a stable cell line of HeLa with the mammalian IPTG-Inducible shRNA PURA knockdown lentiviral vector, purchased in Vector Builder® pLV[shRNA]-LacI:T2A:Puro-U6/2xLacO>hPURA[shRNA#1]. Lentivirus were produced in Hek293T cells by transient co-transfection of the MISSION® Lentiviral Packaging Mix (Sigma®) with 1.35µg of the shRNA-encoding DNA using 7 µg polyethylenimine (PEI, Poliscience®) for transfection of a well from a 6-well plate. Culture supernatants were collected 72 h post-transfection, filtered (0.22 mm filter, cellulose acetate, Ministart®), and supplemented with 8 µg/ml polybrene (Sigma®). Subconfluent HeLa cells ~50.000 in a well from a 6-well plate were infected with the polybrene-supplemented supernatant and 48h post-infection were selected with 1 µg/ml puromycin (sc-108071®) for 1 week.

2_shPURA (IPTG-induced knock-down). HeLa cells from condition 1 were treated with IPTG: isopropyl-galactosidase (TRANS®) 500µM for 72h (replacing medium and IPTG every day)

3_+PURA: PURA overexpression: ~50.000 HeLa cells from condition 1 were transfected with **1.5**µg VB220517-1200nex pRP[Exp]-mCherry/Neo-CMV>hPURA[NM_005859.5] purchased in Vector Builder® using 7 µg polyethylenimine (PEI, Poliscience®). 12hours after, medium was replaced and cells were selected through Geneticin sulfate (G 418_ab144261) 200 µg/ml for 72h.

4_ +GLUT1 (GLUT1 overexpression): ~50.000 HeLa cells from condition 1 were transfected with 1.5 µg pRP[Exp]-Bsd-CAG>hSLC2A1[NM_006516.4] purchased in Vector Builder® using 7 µg polyethylenimine (PEI, Poliscience®). 12hours after, medium was replaced and cells were selected through Blasticidin S hydrochloride, Nucleoside (ab141452) 10 µg /ml for 72h.

5_+GLUT1+shPURA (concomitant GLUT1 overexpression and induced PURA knockdown): cells were treated as condition 4 and during the selection process IPTG was added as in condition 2.

6_+PURA+GLUT1 (PURA and GLUT1 co-overexpression). A combination of condition 3 and 4 was carried out. Both plasmids were transfected simultaneously, and selection was carried out with both antibiotics (Geneticin+ Blasticidin) for 72h.

Glucose uptake assays: HeLa cells from the 6 conditions above, on their second day of selection were seeded in glass coverslips. 24h later, 2-(N-(7-nitro-2,1,3-benzoxadiazol-4-yl)amino)-2-deoxyglucopyranoside (2-NBDG, Medkoo®) was added in DMEM low glucose medium to a 30μM concentration for 1h. Then, cells were washed with PBS and imaged in DMEM FluoroBrite medium using Zeiss Axio Observer fluorescence inverted microscope® or tripsinized and analyzed through BD Accuri C6 Plus Flow Cytometer®, fluorescence being evaluated with channel FL1 (533/30nm). Microscopy fluorescence was evaluated using Image J® software (mean grey value from +50 cells per image ~5 photos per condition substracting background). Flow cytometry assays were analyzed using FloJo v X.0.7® software.

mRNA expression, RTqPCR: RNA was extracted from HeLa cells (conditions 1,2,3) using TriPure® (Roche®) according to manufacturers´ protocol. RNA retrotranscription to obtain cDNA was performed using M-MLV retrotranscriptase (Inbio Highway®) based on manufacturer´s protocol. SYBR based qPCR for genes: PURA, GLUT1 and ACTINB or B2M as housekeeping genes was performed with SsoAdv univer SYBR GRN BioRad®. PURA and GLUT1 reaction parted from 40ng of RNA derived cDNA, housekeeping genes´ reaction from 10ng. Primer concentration for all 4 pairs was 250nM of each. qPCR was carried out with the following thermal program: 95 °C 3 min; 40 cycles of: 95 °C 15 s, 60 °C 30 s (read), 72 °C 30 s using the BioRad PCR CFX96® qPCR equipment. Results were analyzed with CFX Maestro Software®. Quantification was estimated through ΔΔCT method.

Primers´ sequences:

gene	Strand	Sequence 5´-3´
PURA	forward	AAGACACCACCTGTAGGAGC
	reverse	CACACTCAACCAGGGAGCAT
GLUT1	forward	GCGGGTTGTGCCATACTCATGACC
	reverse	AGGCCACAAAGCCAAAGATGGCC
ACTB	forward	TGACGTGGACATCCGCAAAG
	reverse	CTGGAAGGTGGACAGCGAGG
B2M	forward	GACTTGTCTTTCAGCAAGGA
	reverse	ACAAAGTCACATGGTTCACA

Western Blots:

Cells were lysed with lysis buffer solution compatible with Co-Immunoprecipitation assays: 1mM EDTA, 10% glycerol, 75mM NaCl, 0.05% SDS, 100mM Tris-Cl pH 7.4, 0.1% (v/v) triton X-100) and measured through BCA kit (Thermofisher Scientific®). Proteins (10–30 μg) were run on a 10% SDS–polyacrylamide gels and then transferred to a nitrocellulose membrane (Biorad®). The membranes were blocked in 5% lowfat milk-PBS-tween solution and then incubated overnight at 4 °C with primary antibodies: anti-PURA 1:1500 (rabbit—ab125200

abcam®), anti-GLUT1 1:2000 (mouse— [GLUT1/2476] (A249979) Antibodies®) and anti-Vinculin Antibody 1:2000 CAB2752-20 (rabbit—GENIE®) followed by PBS-Tween washes and secondary antibody incubation (2h at room temperature): Horseradish peroxidase secondary antibodies: mouse (Gt anti-mouse IgG -H+L- Invitrogen®) 1:10000 and rabbit (Gt anti-Rb IgG -H+L- Invitrogen®) 1:3000. Bands were developed using chemiluminescence (ECL BPS-Bioscience®), visualized with a LAS Fujifilm 4000 system (GE Healthcare Life Sciences®) and quantified using Image J® software.

Indirect immunofluorescence:

Cells were fixed with 4% Paraformaldehyde solution 30 min at room temperature, following washes with PBS, and then quenched with $ClNH_4$ 50 mM for 30 min at room temperature. Cells were permeabilized with Albumin 2%/Saponin0.1% PBS solution, following which they were incubated with anti-PURA antibody (rabbit—ab125200 abcam®) 1:200 and anti-GLUT1 (mouse-RyD MB14181®) 1:100 or [GLUT1/2476] (A249979) Antibodies®) 1:200, overnight at 4 °C. The primary antibody was rinsed and then cells were incubated with secondary antibodies ab150077 Goat Anti-Rabbit IgG H&L (Alexa Fluor® 488) 1:750 and ab150115 Goat Anti-Mouse IgG H&L (Alexa Fluor® 647) 1:750, washed, and coverslips were mounted on glass slides using Mowiol + Hoescht (LifeTechnologies®) and examined by fluorescence confocal microscopy (Olympus Confocal Microscope FV1000-EVA®).

Dot blot overlay:

A nitrocellulose membrane was imbedded with 1µl of antibodies targeting PURA (rabbit-ab125200 abcam®) or GLUT1 (mouse-RyD MB14181®), blocked with BSA 5% solution 1h room temp, then the exposed to ~ 40µg HeLa cell lysates overnight at 4 °C. Membranes were washed and subsequently exposed to the counterpart protein´s antibody overnight at 4 °C (nitrocellulose membrane that was imbedded with anti-PURA was incubated with anti-GLUT1 and vice versa, 1:500 for anti-PURA and 1:250 for anti-GLUT1 antibodies). Membranes were washed and then incubated with Horseradish peroxidase secondary antibodies against the last antibody: mouse (Gt anti-mouse IgG -H+L- Invitrogen®) 1:10000 and rabbit (Gt anti-Rb IgG -H+L- Invitrogen ®) 1:3000. Dot blots were developed using chemiluminescence (ECL BPS-Bioscience®) and visualized with a LAS Fujifilm 4000 system (GE Healthcare Life Sciences®).

Co-Immunoprecipitation:

Immunoprecipitation was carried out through ImmunoPure Plus Immoblized Protein A agarose beads (PIERCE®) bond to anti-PURA ab125200 abcam® following protocol available at   https://www.abcam.com/protocols/immunoprecipitation-protocol-1.   We   followed method B from the mentioned protocol using 15µl of bead slurry + 0.5 µg of anti-PURA antibody per 30 µg of protein from cell lysate. After thorough washes, beads harboring the pulldown were run on a 10% SDS–polyacrylamide gel and the presence of GLUT1 was analyzed through Western Blot. RNAse A (Thermofisher Scientific®) was used to evaluate RNA dependance of the protein complex PURA:GLUT1. We used 0.5µg RNAse A per 12µl of lysate, 10min 25°C incubation prior to the immunoprecipitation protocol.

Computational methods:

Atomistic molecular dynamics: Atomistic simulations of GLUT1 and PURA in complex were conducted with Gromacs-2023[41]. Proteins were solvated using CHARMM-GUI web server[42]. All protein-protein complexes were minimized and equilibrated following the

CHARMM-GUI protocol for Gromacs[43]. For productions runs the pressure and the temperature were set to 1.0 bar and 303.15K. Pressure was controlled by the Parrinello-Rahman barostat[44].Temperature was controlled by de Nose-Hoover thermostat[45] using a 1ps coupling constant. Cut-offs for van der Waals and electrostatic interactions were set to 1.2nm, using the particle Mesh Ewald (PME) mehtod[46] with Verlet cut-off scheme. In all cases a 4th order LINCS algorithm was applied[47].

Article drafting: we used ChatGPT, an AI-powered language model developed by OpenAI, solely for language-related assistance in the composition of this research paper, with no influence on the content or research outcomes.

Statistics software: Graph Pad Prism v5.03® was used for statistical analyses and graph confection.

Art work: Corel draw 2020® was used to draft figures. Computational figures were prepared with Visual Molecular Dynamics (VMD)[48], Schrödinger academic version, MDVWhole, Grace (GRaphing, Advanced Computation and Exploration of data) and Inkscape. Biorender® was used to graph the plasma membrane in figure 3.

RESULTS

Hypoglycorrhachia: a recurrent finding in PURA syndrome patients

In 2018, our research team reported the inaugural case of a patient exhibiting PURA deficiency with the distinctive manifestation of hypoglycorrhachia[35]. Notably, this patient displayed diminished GLUT1 expression within blood cells. In the present study, we expand upon our previous work by presenting data from an additional cohort of patients, who exhibited as well, the hallmark symptom of hypoglycorrhachia. A comprehensive summary of the key clinical observations for these patients, along with details regarding PURA mutations and the corresponding glycorrhachia levels, as well as the glycorrhachia-to-glycemia ratio, is presented in Table 1.

Table 1

patient	PURA mutation (heterozygosis and *de novo*) Human (GRCh38/hg38) genome	PURA mutant protein	Mean Glycorrhachia (normal value >2.9mM)[40]	Mean Glycorrhachia-to-glycemia ratio (normal value>0.59)[40]	Other clinical aspects	Care center location	Previously reported
1	Chr5: 140114767delA NM_005859.4 c.586delA	p.I196fs*30 (223 aminoacids)	1.6mM	0.39	Hypotonia, seizures, apnea, development delay	Mendoza, Argenitna	Yes [30,35]

2	Chr5: 140114918del TGAGCGA NM_005859.4 c.737_744del	p.V246 Gfs*45 (289 aa)	2.9mM	0.44	Hypotonia, seizures, development delay	Buenos Aires, Argentina	No
3	Chr5: 140114992del TTC NM_005859.4 c.810_812 delTTC	p.F271 del (321aa)	2.1mM	0.55	Hypotonia, seizures, apnea, development delay	Rome, Italy	No
4	Chr5: 140114714dup TGGCCTGGGCTCC NM_005859.4 c.534_546dup TGGCCTGGGCTCC	p.T183 Wfs*22 (203aa)	2.2mM	0.44	Hypotonia, seizures, development delay	Rome, Italy	No
5	Chr5: 140114386C>T NM_005859.4 c.205C>T	p.Q69* (68aa)	2.3mM	0.42	Hypotonia, seizures, development delay	Rome, Italy	No
6	Chr5: 140114778del TTC NM_005859.4 c.697_699 delTTC	p.F233 del (321aa)	2.2mM	0.47	Hypotonia, seizures, development delay, hyperprolactinemia	Melbourne, Australia	Yes[26,30]

Table 1 presents a cohort of individuals diagnosed with PURA syndrome manifesting hypoglycorrhachia. The table includes information on DNA and mRNA mutations, protein consequences, glycorrhachia levels, and the corresponding glycorrhachia/glycemia ratios. Additionally, the table summarizes key clinical features associated with the presented cases.

An intriguing observation stemming from our analysis is the consistent association between hypoglycorrhachia and specific PURA mutations affecting the PUR III repeat region within the protein's structure domain which is believed to facilitate interactions with other proteins [3]. In light that hypoglycorrhachia could now be considered a new finding in patients with PURA deficiency and observing that the rest of the clinical features overlap, we ventured to take these clinical findings to the bench side and investigate a functional connection between PURA and GLUT1.

PURA enhances glucose uptake in cultured HeLa cells by potentiating the function of GLUT1, without inducing significant alterations in GLUT1 expression levels.

Firstly, we wanted to prove in an *in vitro* model a functional interplay between these proteins. Accordingly, glucose uptake served as the ultimate metric to assess the influence of PURA on GLUT1's functionality.

PURA was originally delineated in HeLa cells[2], and as a result, we devised our experimental setup utilizing these cells as our chosen model system. We established a stable HeLa cell line containing an inducible shRNA targeting the PURA gene. These cells were manipulated to either suppress PURA expression (via IPTG shRNA induction) or augment PURA expression (via transient transfection with a PURA expression plasmid). In addition, we used GLUT1 overexpression as a positive control. To discern the critical role of PURA in glucose uptake and its interrelationship with GLUT1, we devised six distinct conditions as follows: 1_Control (PURA baseline), 2_ shPURA (IPTG-induced PURA knockdown), 3_ +PURA (PURA overexpression), 4_ +GLUT1 (GLUT1 overexpression), 5_+GLUT1+shPURA (concomitant GLUT1 overexpression and induced PURA knockdown), 6_+PURA+GLUT1 (PURA and GLUT1 co-overexpression). We validated the precision of the proposed manipulations by Western Blot. (Fig.1A)

To evaluate glucose uptake across these six conditions, we employed a fluorescent glucose analog, 2-deoxy-2-[(7-nitro-2,1,3-benzoxadiazol-4-yl)amino]-D-glucose (2-DNBG). Subsequently, we quantified fluorescence levels utilizing both fluorescent microscopy (Fig.1B) and flow cytometry techniques (Fig. 1C).

Our findings revealed that PURA upregulation significantly enhanced glucose uptake, comparable to the impact of sole GLUT1 overexpression, as visually depicted in microscopy (Fig.1B, condition 3) and vindicated through flow cytometry (Fig.1C). Conversely, PURA knockdown exerted a diminishing effect on glucose uptake, evident in basal conditions as well as in cells with heightened GLUT1 expression, as illustrated in microscopy (Fig.1B, conditions 2 and 5). These experiments show that PURA is a major exponent for glucose uptake and particularly condition 5′s result (diminished glucose uptake when PURA is knocked down in a high GLUT1 cellular environment) shows a functional interdependence of GLUT1 towards PURA, indicating a solid interplay between these two proteins. In addition, the absence of synergy in glucose uptake under condition 6 (overexpression of both proteins) indicates that PURA and GLUT1 function in the same pathway for glucose incorporation.

Given PURA's established capability to modulate gene transcription and translation, and the finding of diminished GLUT1 expression in blood cells from a patient with PURA syndrome[35], firstly, we thought that PURA might regulate GLUT1′s transcription and/or translation. To evaluate this, we conducted a focused examination of GLUT1 mRNA and protein expression levels during instances of PURA up and downregulation (Fig. 1D). Notably, these experimental manipulations did not yield significant alterations in GLUT1 levels, leaving us to investigate other possibilities of partnership between the proteins. Taking into account that the PUR III repeat domain is known to facilitate interactions with other proteins[3], what if PURA and GLUT1 were to interact in a complex?
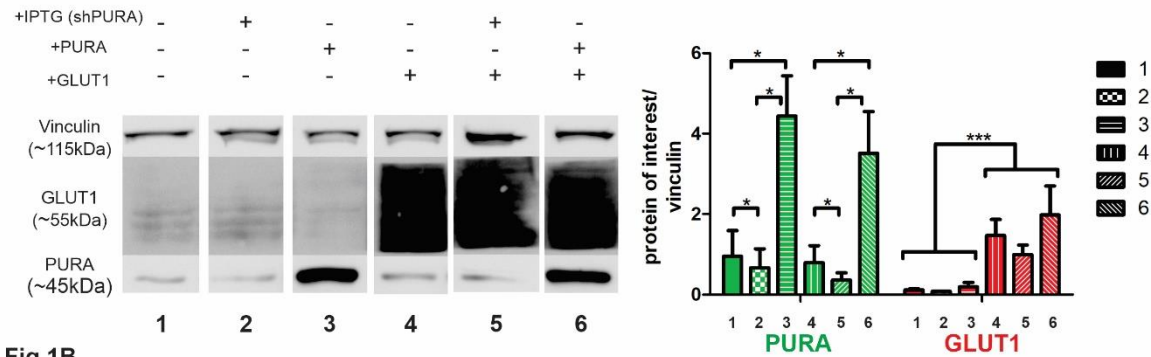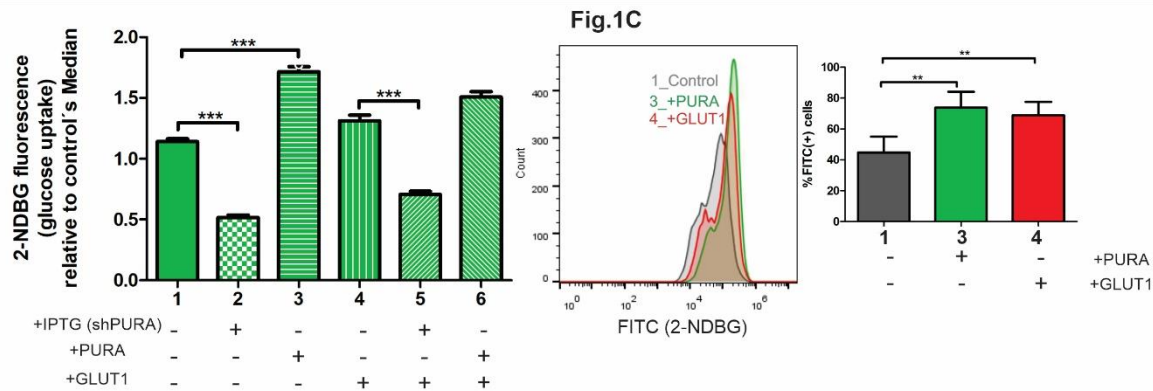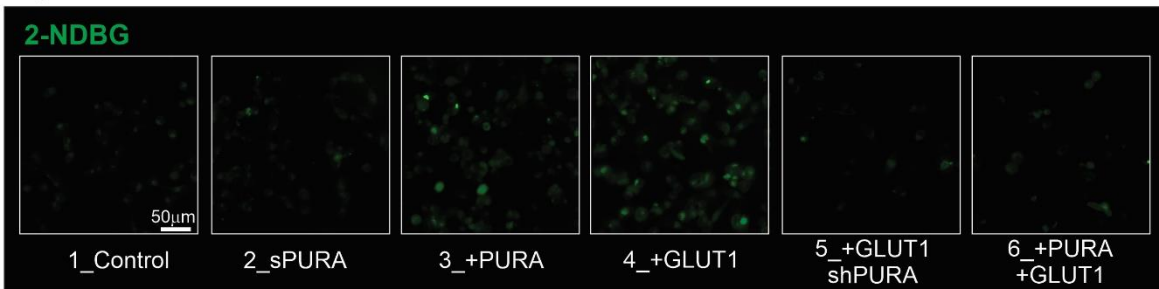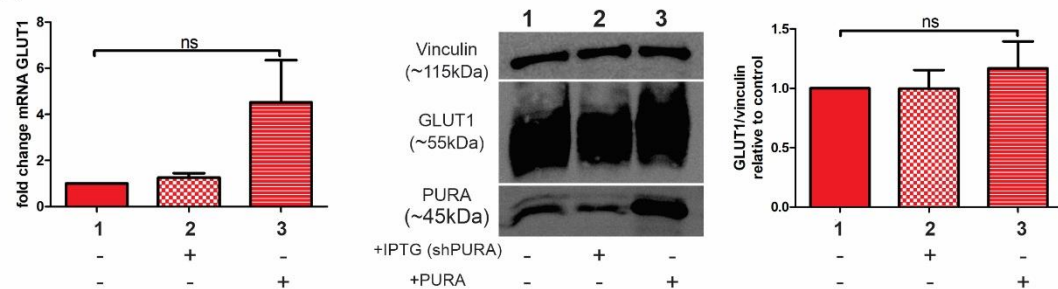
Figure 1: *PURA enhances glucose uptake in cultured HeLa cells without inducing significant alterations in GLUT1 expression levels*. **1A.** Validation by Western Blot of the proposed expression manipulation of PURA and GLUT1. 1_Control (PURA baseline), 2_ shPURA (IPTG-induced PURA knockdown), 3_ +PURA (PURA overexpression), 4_ +GLUT1 (GLUT1 overexpression), 5_+GLUT1+shPURA (concomitant GLUT1 overexpression and induced PURA knockdown), 6_+PURA+GLUT1 (PURA and GLUT1 co-overexpression). All lanes correspond to the same gel but have been cut in order to follow the 1 to 6 conditions´ order N=3. PURA*p<0.05. One-tailed paired student´s T-test; GLUT1: ***p<0.001 Two-tailed paired Student´s T test between all conditions with basal GLUT1 level

(conditions 1,2,3) and all conditions with GLUT1 overexpression (conditions 4,5,6). **1B and C.** Glucose uptake assay using the fluorescent glucose analog, 2-deoxy-2-[(7-nitro-2,1,3-benzoxadiazol-4-yl)amino]-D-glucose (2-NDBG). We quantified fluorescence levels with fluorescent microscopy (**1B:** Glucose uptake was different in all six conditions except 3 vs 6, Kruskal-Wallis test, Dunn´s Multiple Comparison post-test. Significance was p<0.01 for all significant comparisons. We have selectively displayed on the graph only those comparisons that are most pertinent to convey the core message of this paper, ***p<0.001); and flow-cytometry (**1C**, **p<0.01 One-way ANOVA+ Tukey's Multiple Comparison Test). **1D.** GLUT1 expression was measured at an mRNA level through SYBR based qPCR, Δ ΔCT quantification method (left panel) and at a protein level through Western Blot (right side), One-way ANOVA+ Tukey's Multiple Comparison Test. ns: not significant.

PURA and GLUT1 are observed to engage in a cellular complex independently of RNA interactions.

In light of the fact that the functional association between PURA and GLUT1 did not appear to hinge on the abundance of GLUT1, we embarked on investigating the potential formation of a physical complex between these two proteins.

Through our experiments we revealed several lines of evidence that support the notion of a physical interaction between PURA and GLUT1:

Immunofluorescence microscopy revealed co-localization of PURA and GLUT1 within HeLa cells (Fig. 2A). This co-localization was more pronounced when both proteins were concurrently overexpressed or when PURA overexpression was coupled with indirect GLUT1 upregulation with rotenone (mitochondrial complex 1 inhibitor) treatment 10µM 24h(mean Pearson´s coefficient 0.81: Supplementary material Fig. S1A and S1B). [49,50].

Dot-blot overlay assays yielded additional evidence of the interaction between PURA and GLUT1. A nitrocellulose membrane was imbedded with the antibody targeting PURA (Fig 2B., left panel) or GLUT1 (Fig. 2B, right panel) and then exposed to HeLa cell lysates overexpressing PURA. As a result, these antibodies effectively captured and immobilized the respective counterpart protein upon the nitrocellulose membrane, adding further evidence for PURA-GLUT1 interaction (Fig. 2B).

Co-immunoprecipitation experiments were conducted using anti-PURA antibody conjugated to Protein A agarose beads. Proteins from cell lysates overexpressing PURA were exposed to the immune-anti-PURA-coated beads. The pull-down was isolated and subsequently analyzed by Western Blot, confirming the presence of GLUT1 in the pull-down (Fig. 2C, left panel). Importantly, this interaction persisted even when PURA levels were reduced through knockdown, providing compelling evidence for its persistence under conditions of diminished PURA expression (Supplementary Material Fig. 2S). Accordingly, we can affirm that PURA and GLUT1 interact with each other. However, this interaction could be direct or indirect.

Considering PURA's well-established role as an RNA-binding protein primarily involved in the formation of ribonucleoprotein (RNP) complexes, we asked ourselves if this interaction could be mediated by RNA. Therefore, we introduced a condition wherein lysates were pretreated with RNAse A. Remarkably, this treatment did not alter the quantity of GLUT1 detected in the pulled-down complexes (Fig. 2B, right panel). This finding suggests an RNA-independent interaction between PURA and GLUT1.
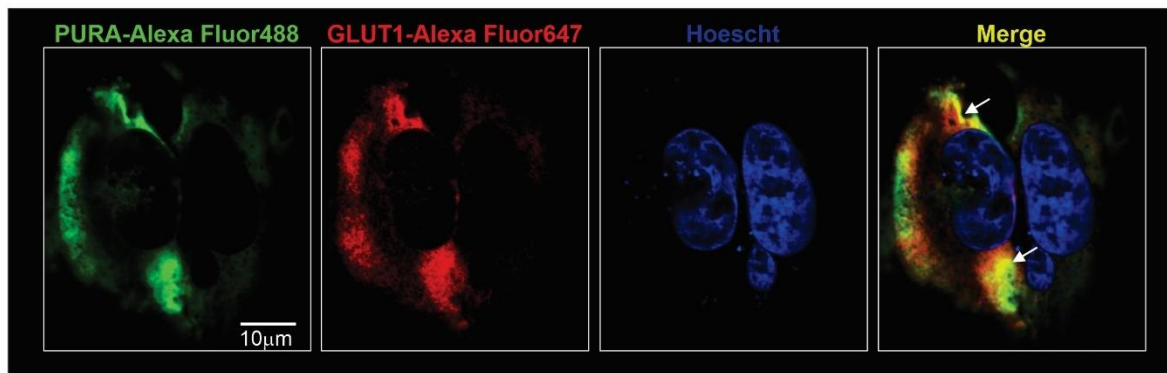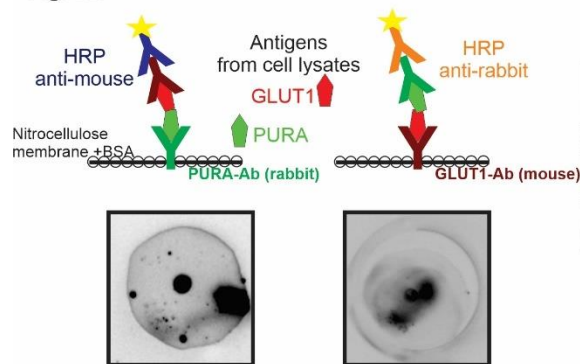
Figure 2.

Fig. 2A

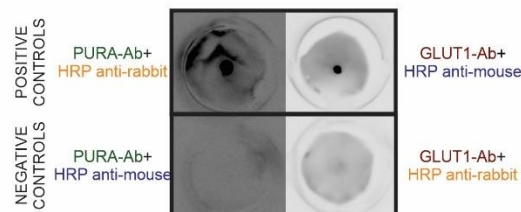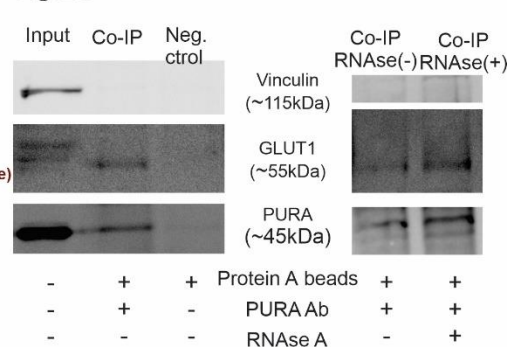
Fig. 2B

Fig. 2C

Figure2: PURA and GLUT1 form a complex: 2A: Confocal Immunofluorescence Microscopy. Confocal laser micrographs depict indirect immunofluorescence staining of PURA (labeled with AlexaFluor 488 in green) and GLUT1 (labeled with AlexaFluor 647 in red) within HeLa cells overexpressing PURA and treated with Rotenone to enhance GLUT1 expression. The cell nuclei were stained with Hoescht (blue). Colocalization of the two proteins in the merged image is represented as yellow, indicated by white arrows. **2B**: Dot Blot Overlay Assay. PURA (left panel) and GLUT1 (right panel) antibodies were imbedded in the center of circular pieces of nitrocellulose membrane, BSA was used to block non-specific interaction. HeLa cell lysates from cells overexpressing PURA were exposed to the membrane and subsequently washed. Following this, the membrane was incubated with antibodies targeting the counterpart protein, followed by secondary antibody incubation with horseradish peroxidase (HRP) reaction visualization. Controls are shown in the bottom of the figure. Positive and negative controls were processed similarly, excluding incubation with cell lysates, to demonstrate antibody specificity. Notably, PURA antibodies are of rabbit origin, while GLUT1 antibodies are of mouse origin, allowing for their differentiation based on the secondary antibody's signal. **2C**. Co-immunoprecipitation of GLUT1 and PURA using Protein A agarose beads bond to anti-PURA antibody. The left panel demonstrates the presence of GLUT1 in the pull-down fraction associated with Protein A agarose beads and anti-PURA antibody (Ab), while it is absent in the pull-down from beads lacking anti-PURA Ab. The right panel reveals that treatment

with RNAse does not influence the pull-down of GLUT1 facilitated by PURA-Protein A beads, suggesting that their interaction is not mediated by RNA.

PURA mutations identified in patients displaying hypoglycorrhachia were found to exhibit altered protein-protein affinity, as through computational analysis.

With no crystallographic structure still available for PURA (Uniprot: Q56A79), we used AlphaFold[51] as a starting point for its computational structural prediction. Figure 3 shows the resulting PURA´s structure (res 57-322), the first 56 residues are predicted to be disordered and were deleted from the figure to make it visually more comprehensive. Additionally, to account for the PDZ binding motif in GLUT1 (res 488-492, DSQV), we also used AlphaFold to predict missing residues in the original crystal structure of the human sugar transporter GLUT1 (PDB ID: 6THA) [52,53]. Figure 3 shows full-length GLUT1 (res 1-492). PURA´s unstructured N-terminal was deleted before computational analysis. Initial binding sites for docking in PURA and GLUT1 were selected at the middle of Repeat-III region (res 270-300) and at the C-terminal PDZ binding motif (res 488-492), respectively and according to previous experimental studies that predict the PURA PURIII domain and the GLUT1 PDZ domain as the main protein-protein interacting regions[3,54] (Fig 3).
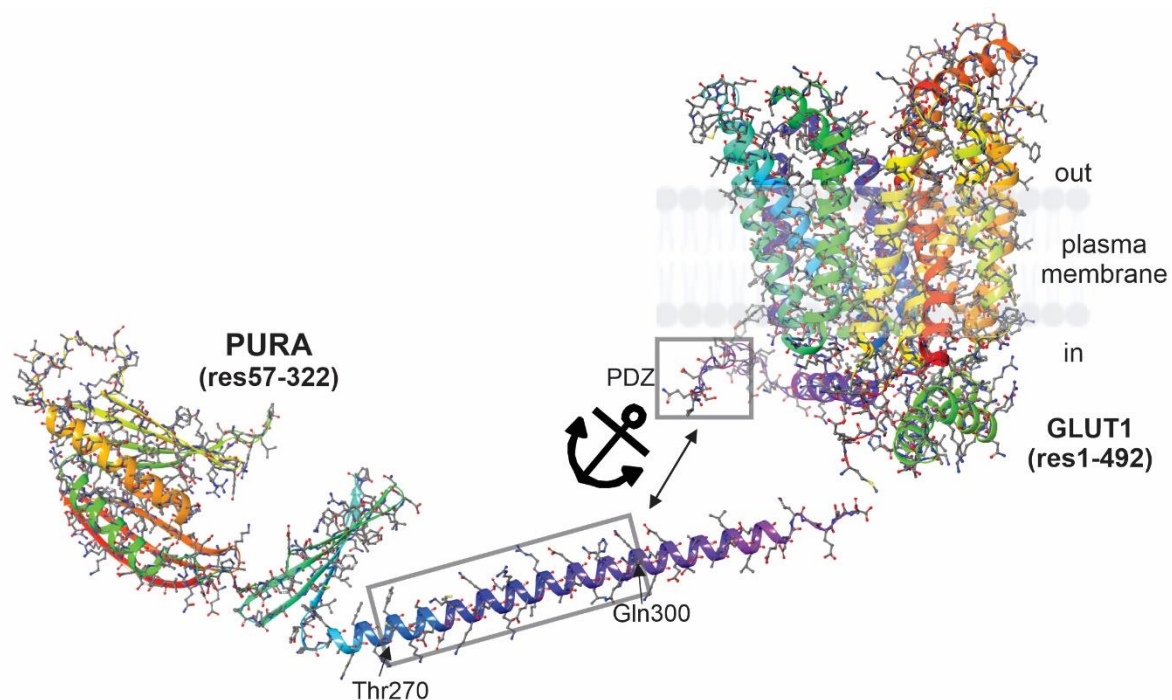

Figure 3: AlphaFold protein predictions. Left: wild-type PURA (res. 57-322). Right: GLUT1 including the PDZ binding motif (res 488-492, DSQV). Both proteins are rainbow-colored from N-terminal to C-terminal (from red to violet). Grey squares frame the regions from both proteins that were used as initial binding sites for docking purposes: PURA: Thr270-Gln300; GLUT1: PDZ motif: res. 488-492. Anchor + double-headed arrow is meant to point out the proposed docking region.

Protein-protein complexes were constructed via molecular docking with the ZDOCK server[55,56]and refined using atomistic molecular dynamics to account for full flexibility of the docking-generated PURA:GLUT1 complexes[57–59] using Gromacs-2023[41,60].

Four PURA versions (wild-type + 3 mutants) in complex with GLUT1 were studied, as detailed below (mutations are shown in red):

(i) wild-type PURA (res 57-322):
ETQELASKRVDIQNKRFYLDVKQNAKGRFLKIAEVGAGGNKSRLTLSMSVAVEFRDYLGDFIEHYAQLGP
SQPPDLAQAQDEPRRALKSEFLVRENRKYYMDLKENQRGRFLRIRQTVNRGPGLGSTQGQTIALPAQG
LIEFRDALAKLIDDYGVEEEPAELPEGTSLTVDNKRFFFDVGSNKYGVFMRVSEVKPTYRNSITVPYKVWA
KFGHTFCKYSEEMKKIQEKQREKRAACEQLHQQQQQQQEETAAATLLLQGEEEGEED
(ii) PURA-mut 1 (res 57-223):
ETQELASKRVDIQNKRFYLDVKQNAKGRFLKIAEVGAGGNKSRLTLSMSVAVEFRDYLGDFIEHYAQLGPS
QPPDLAQAQDEPRRALKSEFLVRENRKYYMDLKENQRGRFLRIRQTVNRGPGLGSTQGQTIALPAQGLS
SSVTLWPSSSTTTEWRRSRPSCPRAPP
(iii) PURA-mut 2 (res 57-289):
MADRDSGSEQGGAALGSGGSLGHPGSGSGSGGGGGGGGGGGGGSGGGGGGAPGGLQHETQELASK
RVDIQNKRFYLDVKQNAKGRFLKIAEVGAGGNKSRLTLSMSVAVEFRDYLGDFIEHYAQLGPSQPPDLA
QAQDEPRRALKSEFLVRENRKYYMDLKENQRGRFLRIRQTVNRGPGLGSTQGQTIALPAQGLIEFRDAL
AKLIDDYGVEEEPAELPEGTSLTVDNKRFFFDVGSNKYGVFMRGEAHLSQLHHRALQGVGQVRTHLLQ
VLGGDEEDSREAEGEAGCL
(iv) PURA-mut 3 (res 57-322, Phe271 deleted):
ETQELASKRVDIQNKRFYLDVKQNAKGRFLKIAEVGAGGNKSRLTLSMSVAVEFRDYLGDFIEHYAQLGP
SQPPDLAQAQDEPRRALKSEFLVRENRKYYMDLKENQRGRFLRIRQTVNRGPGLGSTQGQTIALPAQG
LIEFRDALAKLIDDYGVEEEPAELPEGTSLTVDNKRFFFDVGSNKYGVFMRVSEVKPTYRNSITVPYKVWA
KFGHT_CKYSEEMKKIQEKQREKRAACEQLHQQQQQQQEETAAATLLLQGEEEGEED

Ranked complexes according to ZDOCK scoring function were visually inspected and a single protein-protein complex was selected for each one of the four PURA variants studied here. As a practical measure of protein-protein stability we estimated the total amount of potential donor-acceptor hydrogen bond pairs and the effective steady-state H-bonds formed at the protein-protein interface during the simulation[61,62], see Table 2.

Table 2

PURA variant	Predicted H-donors	Predicted H-acceptors	steady-state H-bonds
wild-type	1076	2087	33
mut 1	939	1785	34
mut 2	1022	1980	19
mut 3	1075	2085	20

Table2. Protein-protein PURA variants: GLUT1 complex stability parameters: Predicted H-donors and acceptors plus established steady-state-H-bonds during simulation.
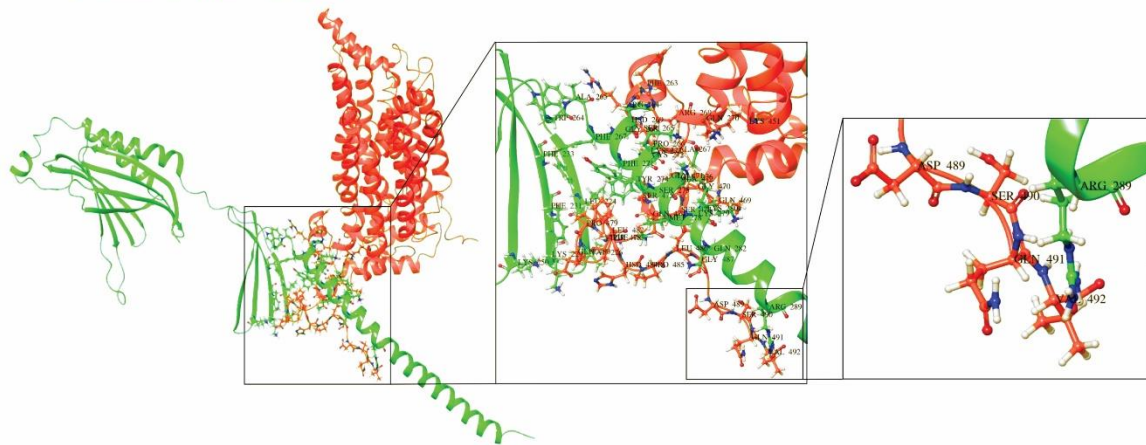
Table 2 suggests that PURA(wild-type) and PURA(mut 3) may establish the most amounts of interface H-Bonds, followed by PURA(mut 2) and PURA(mut 1), in agreement with the truncation lengths (at 289 and 223, respectively). However, the effective amount of hydrogen bonds that form within the protein-protein interface is significantly higher for PURA(wild-type) than for PURA(mut 3) even though PURA(mut 3) differs only in one deleted amino acid (Phe271). The protein-protein affinity is drastically reduced, giving the deleted Phe271 right at the beginning of the alpha-helix in the Repeat-III PURA region, a strategic location for the interaction with the GLUT1's C-terminal PDZ binding domain. PURA(mut 2), which generates a mutated-truncated 289-amino acid version, reduces its affinity for GLUT1 in a third and interacts with GLUT1 amino acids between positions 445-451 (not the PDZ-binding motif).

PURA(mut.1) although truncated at 223, and even with the total absence of the Repeat-III region established as much as interface H-bonds as the wild-type protein, however, through PURA residues far away from the normally proposed PURIII-PDZ interaction (PURA-Glu57, Thr58, Asn80 and Lys82). Taking into account that the patient carrying mut 1 (Patient 1) clinically seems to have the least functional GLUT1, this abnormal and stable interaction could be adding a negative dominant effect for this mutation.
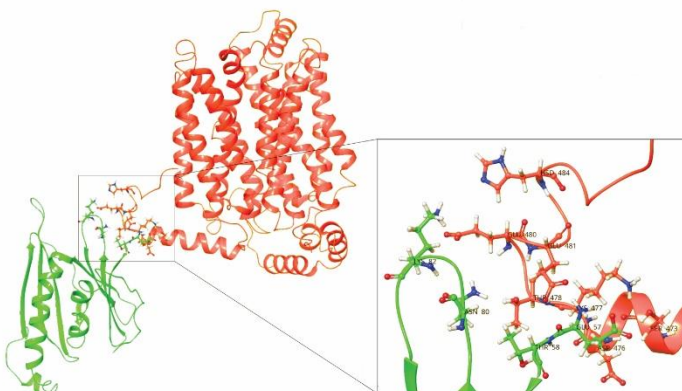
See figure 4 for final molecular dynamics snapshots and residues involved at each protein-protein interface.
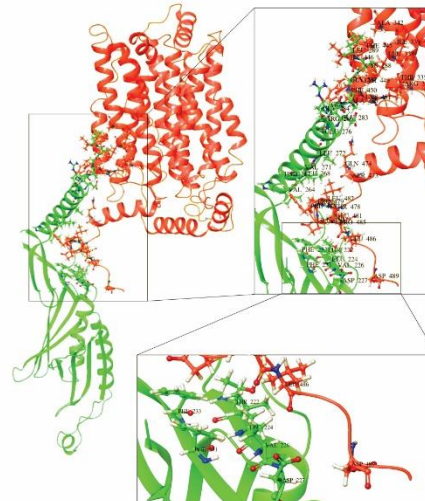
Figure 4.

A. PURA wild-type : GLUT1

B. PURA mut.1: GLUT1

C. PURA mut.2: GLUT1
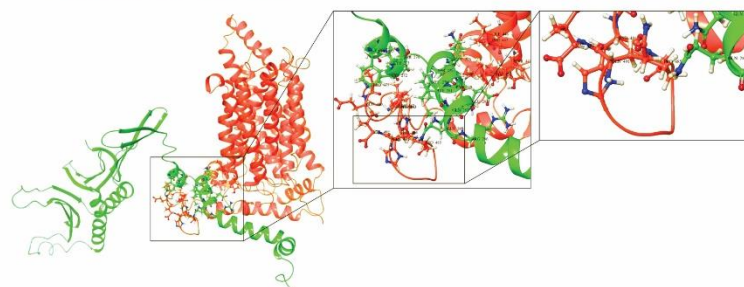
D. PURA mut.3: GLUT1

Figure 4. Molecular dynamics snapshots and residues involved at each protein-protein interface. PURA protein in green, GLUT1 in red. First zoom-in: PURA:GLUT1 interface, second zoom-in: PURA-GLUT1 PDZ interface. **4A.** PURA wild-type: GLUT1. PURIII repeat interacting with GLUT1´s PDZ binding domain, as expected. **4B**: PURA-mutant 1 (PUR repeat I) interacting with GLUT1(not involving PDZ binding motif). **4C**: PURA mutant 2 (abnormal PURIII) interacting with GLUT1´ PDZ binding domain. **4D**: PURA-mutant 3 (abnormal PURIII) interacting with GLUT1 (not involving PDZ binding motif). Corey–Pauling–Koltun coloring for atoms: white for hydrogen, blue for nitrogen, red for oxygen.

DISCUSSION

Our study delves into the multifaceted roles of PURA, a protein with a well-established involvement in cellular processes across various cellular domains. PURA's intricate functions have garnered considerable attention in the past years due to its association with neurological disorders and genetic syndromes.

The identification of hypoglycorrhachia as a consistent clinical feature in PURA syndrome, first reported by our team in 2018, raised questions regarding the molecular basis of this phenomenon. Here, we have extended our investigation to include a cohort of new patients exhibiting this hallmark symptom, shedding light on a potential regulatory role of PURA in glucose homeostasis through GLUT1.

Intriguingly, our functional experiments revealed a novel, fundamental role for PURA in cellular glucose uptake. The increase in glucose intake when PURA is upregulated (*no different from GLUT1´s upregulation effect*) and its diminishment upon PURA knockdown even in the presence of high GLUT1 levels suggests that GLUT1´s function strongly depends on PURA. These findings implicate PURA as a previously unrecognized factor in glucose transport, indicating its potential role in fine-tuning cellular glucose homeostasis and serves to explain the clinical observations in the 6 included PURA-patients described in this paper.

While PURA's well-established role as a transcriptional and translational modulator led us to consider an impact on GLUT1's expression, our experiments provided evidence that this was not their way for interplay. Our work supports the idea of a PURA:GLUT1 complex formation to explain the their interdependent function.

Being GLUT1 a plasma membrane protein, with 12 transmembrane domains[52] its degradation and recycling depends on vesicular transportation. It has been described to enter the endocytic pathway and is recycled as a retromer-mediated cargo[49,63]. Knock-out of the well-established endocytic GTPase Rab21 disrupts GLUT1 recycling and decreases glucose uptake in HeLa cells[63]. Furthermore, GLUT1 has been shown to interact with Myosin 6 and the kinesin superfamily protein KIF-1B via its transporter binding protein GLUT1CBP (GLUT1 transporter binding protein) [64,65], probably having an important role in recycling of the glucose transporter and specific localization to the plasma membrane for its functioning. On the other hand, PURA is also known to closely associate with motor proteins[1]. The cargo transporting conventional kinesin KIF5[20] and myosin Myosin 5a[19,66] have been found to interact with PURA. Given these facts, one could speculate that PURA could play a role in GLUT1´s trafficking and specific localization for correct functioning. Location of glucose transporters on the plasma membrane are not random[67] and specially when one is talking about the blood-brain-barrier[38,68]. The implications of our results extend beyond the cellular context. We propose that the interplay between PURA and GLUT1 may have broader physiological consequences, potentially influencing glucose transport across the blood-brain barrier.

In conclusion, our study uncovers a previously unrecognized role for PURA in glucose uptake regulation and establishes a functional and physical interaction between PURA and GLUT1. These findings provide valuable insights into the molecular basis of hypoglycorrhachia in PURA-related neurodevelopmental disorder and suggest a potential regulatory role of PURA in glucose homeostasis.

Our results warrant further investigations into the specific cellular compartments of interaction and functional interplay between PURA and GLUT1. Additionally, it is imperative to explore the structural and functional implications of PURA mutations, particularly in the context of GLUT1 interactions.

Author contributions LM conducted the research project. RC performed the wet lab experiments with the help of LM. DMas carried out the computational methods and analyses. CM, MA and DMar provided clinical data from patients. LM wrote the paper with the help of DMas for computational sections. All authors read and approved the final manuscript.

Supplementary material
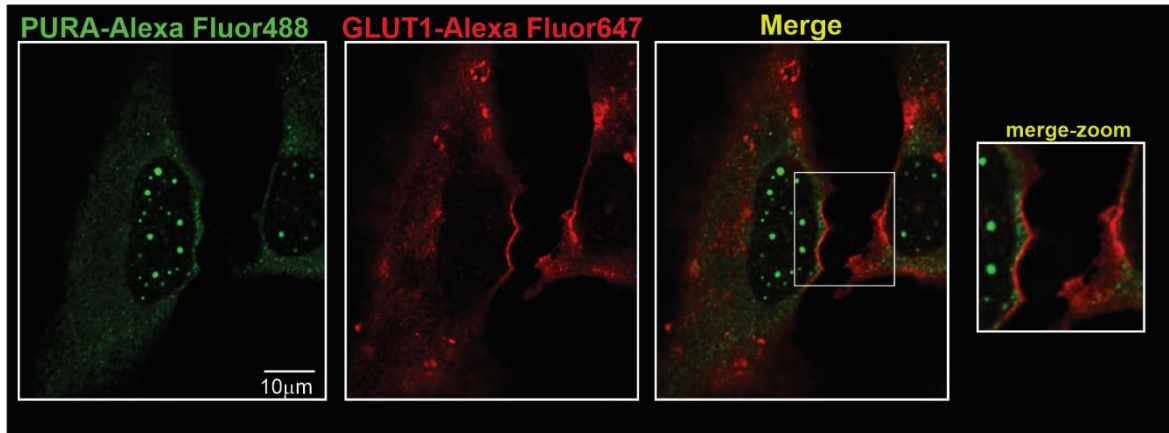
Figure. S1
Fig. S1A

Fig. S1B

Fig. S2

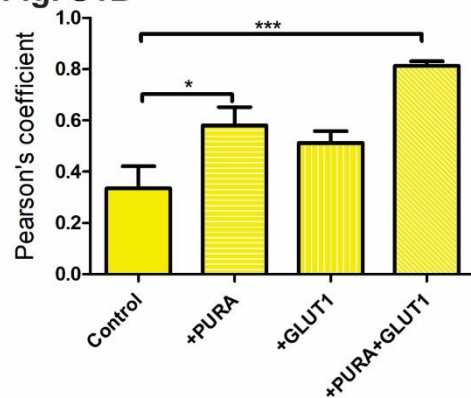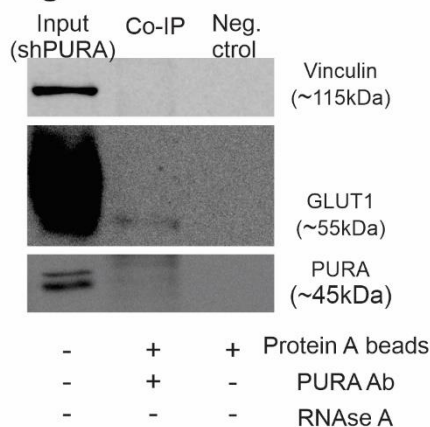**Figure S1A**: Confocal Immunofluorescence Microscopy. Confocal laser micrographs depict indirect immunofluorescence staining of PURA (labeled with AlexaFluor 488 in green) and GLUT1 (labeled with AlexaFluor 647 in red) within HeLa cells overexpressing PURA and GLUT1 expression. Colocalization of the two proteins in the merged image is represented as yellow, zoomed in a white square. **S1B**: Pearson´s coefficients

values from 3 controls, 6 +PURA, 3 +GLUT1, 9 +PURA+GLUT1 photos (3+PURA +Rotenone, 6 +PURA+GLUT1). *** p<0.001, *p<0.05. One-way ANOVA+ Dunnett's Multiple Comparison Test.

Figure S2: Co-immunoprecipitation of GLUT1 and PURA using Protein A agarose beads bond to anti-PURA antibody. shPURA input was used for the pull-down. There is presence of GLUT1 in the pull-down fraction of cells with down-regulated PURA. Anyhow, note that it appears when GLUT1 is overexposed, noting that a small fraction of GLUT1 is being able to bind to the scarce PURA protein.

REFERENCES

[1]   Molitor L, Bacher S, Burczyk S, Niessing D. The Molecular Function of PURA and Its Implications in Neurological Diseases. Front Genet 2021;12. doi:10.3389/fgene.2021.638217.

[2]   Bergemann a D, Johnson EM. The HeLa Pur factor binds single-stranded DNA at a specific element conserved in gene flanking regions and origins of DNA replication. Mol Cell Biol 1992;12:1257–65. doi:10.1128/MCB.12.3.1257.

[3]   Johnson EM, Daniel DC, Gordon J. The pur protein family: Genetic and structural features in development and disease. J Cell Physiol 2013;228:930–7. doi:10.1002/jcp.24237.

[4]   Niessing D. X-ray structure of Pur- ⌣ reveals a Whirly-like fold and an unusual nucleic-acid binding surface 2009;106.

[5]   Weber J, Bao H, Hartlmüller C, Wang Z, Windhager A, Janowski R, et al. Structural basis of nucleic-acid recognition and double-strand unwinding by the essential neuronal protein Pur-alpha. Elife 2016;5:1–23. doi:10.7554/eLife.11297.001.

[6]   Haas S, Gordon J, Khalili K. A developmentally regulated DNA-binding protein from mouse brain stimulates myelin basic protein gene expression. Mol Cell Biol 1993;13:3103–12. doi:10.1128/MCB.13.5.3103.Updated.

[7]   Haas S, Thatikunta P, Steplewski A, Johnson EM, Khalili K, Amini S. A 39-kD DNA-binding protein from mouse brain stimulates transcription of myelin basic protein gene in oligodendrocytic cells. J Cell Biol 1995;130:1171–9. doi:10.1083/JCB.130.5.1171.

[8]   Haas S, Steplewski A, Siracusa LD, Amini S, Khalili K. Identification of a sequence-specific single-stranded DNA binding protein that suppresses transcription of the mouse myelin basic protein gene. J Biol Chem 1995;270:12503–10. doi:10.1074/jbc.270.21.12503.

[9]   Steplewski A, Krynska B, Tretiakova A, Haas S, Khalili K, Amini S. MyEF-3, a developmentally controlled brain-derived nuclear protein which specifically interacts with myelin basic protein proximal regulatory sequences. Biochem Biophys Res Commun 1998;243:295–301. doi:10.1006/bbrc.1997.7821.

[10]   Darbinian N, Sawaya BE, Khalili K, Jaffe N, Wortman B, Giordano A, et al. Functional interaction between cyclin T1/cdk9 and Purα determines the level of TNFα promoter activation by Tat in glial cells. J Neuroimmunol 2001;121:3–11. doi:10.1016/S0165-5728(01)00372-1.

[11]   Penberthy WT, Zhao C, Zhang Y, Jessen JR, Yang Z, Bricaud O, et al. Pur alpha and Sp8 as opposing regulators of neural gata2 expression. Dev Biol 2004;275:225–34.

doi:10.1016/J.YDBIO.2004.08.007.

[12]   Darbinian N, Gallia GL, Kundu M, Shcherbik N, Tretiakova A, Giordano A, et al. Association of Purα and E2F-1 suppresses transcriptional activity of E2F-1. Oncogene 1999;18:6398–402. doi:10.1038/sj.onc.1203011.

[13]   Interaction between the pura and E2F-1 transcription factors - PubMed n.d. https://pubmed.ncbi.nlm.nih.gov/15517862/ (accessed September 8, 2023).

[14]   Daigle JG, Krishnamurthy K, Ramesh · Nandini, Casci I, Monaghan J, Mcavoy K, et al. Pur-alpha regulates cytoplasmic stress granule dynamics and ameliorates FUS toxicity. Acta Neuropathol 2016;131:605–20. doi:10.1007/s00401-015-1530-0.

[15]   Tretiakova A, Gallia GL, Shcherbik N, Jameson B, Johnson EM, Amini S, et al. Association of Purα with RNAs homologous to 7 SL determines its binding ability to the myelin basic protein promoter DNA sequence. J Biol Chem 1998;273:22241–7. doi:10.1074/jbc.273.35.22241.

[16]   Kaminski R, Cheeseboro L, Amini S, Johnson EM, White MK, Khalili K, et al. Role of Purα in the cellular response to ultraviolet-C radiation. Cell Cycle 2010;9:4164–73. doi:10.4161/CC.9.20.13456.

[17]   Romano G, Giordano A. Purα and nucleotide excision repair system: Implications in cellular response to ultraviolet C radiation-induced DNA damage and chemoresistance in malignant cells. Cell Cycle 2010;9:4266–4265. doi:10.4161/cc.9.21.13605.

[18]   Johnson EM, Kinoshita Y, Weinreb DB, Wortman MJ, Simon R, Khalili K, et al. Role of Pur alpha in targeting mRNA to sites of translation in hippocampal neuronal dendrites. J Neurosci Res 2006;83:929–43. doi:10.1002/JNR.20806.

[19]   Ohashi S, Koike K, Omori A, Ichinose S, Ohara S, Kobayashi S, et al. Identification of mRNA/protein (mRNP) complexes containing Puralpha, mStaufen, fragile X protein, and myosin Va and their association with rough endoplasmic reticulum equipped with a kinesin motor. J Biol Chem 2002;277:37804–10. doi:10.1074/JBC.M203608200.

[20]   Kanai Y, Dohmae N, Hirokawa N. Kinesin transports RNA: Isolation and characterization of an RNA-transporting granule. Neuron 2004;43:513–25. doi:10.1016/j.neuron.2004.07.022.

[21]   Carlini LE, Getz MJ, Strauch AR, Kelm RJ. Cryptic MCAT enhancer regulation in fibroblasts and smooth muscle cells: Suppression of TEF-1 mediated activation by the single-stranded DNA-binding proteins, Purα, Purβ, and MSY1. J Biol Chem 2002;277:8682–92. doi:10.1074/jbc.M109754200.

[22]   Boivin M, Willemsen R, Hukema RK, Sellier C. Potential pathogenic mechanisms underlying Fragile X Tremor Ataxia Syndrome: RAN translation and/or RNA gain-of-function? Eur J Med Genet 2018;61:674–9. doi:10.1016/J.EJMG.2017.11.001.

[23]   Jin P, Duan R, Qurashi A, Qin Y, Tian D, Rosser TC, et al. Pur alpha binds to rCGG repeats and modulates repeat-mediated neurodegeneration in a Drosophila model of fragile X tremor/ataxia syndrome. Neuron 2007;55:556–64. doi:10.1016/J.NEURON.2007.07.020.

[24]   Wortman MJ, Dagdanova A V., Clark AM, Godfrey EW, Pascal SM, Johnson EM, et al. A synthetic Pur-based peptide binds and alters G-quadruplex secondary structure present in the expanded RNA repeat of C9orf72 ALS/FTD. Biochim Biophys Acta - Mol Cell Res

2020;1867:1–11. doi:10.1016/j.bbamcr.2020.118674.

[25]   Swinnen B, Bento-Abreu A, Gendron TF, Boeynaems S, Bogaert E, Nuyts R, et al. A zebrafish model for C9orf72 ALS reveals RNA toxicity as a pathogenic mechanism. Acta Neuropathol 2018;135:427–43. doi:10.1007/S00401-017-1796-5.

[26]   Hunt D, Leventer RJ, Simons C, Taft R, Swoboda KJ, Gawne-Cain M, et al. Whole exome sequencing in family trios reveals de novo mutations in PURA as a cause of severe neurodevelopmental delay and learning disability. J Med Genet 2014;51:806–13. doi:10.1136/jmedgenet-2014-102798.

[27]   Lalani SR, Zhang J, Schaaf CP, Brown CW, Magoulas P, Tsai ACH, et al. Mutations in PURA cause profound neonatal hypotonia, seizures, and encephalopathy in 5q31.3 microdeletion syndrome. Am J Hum Genet 2014;95:579–83. doi:10.1016/j.ajhg.2014.09.014.

[28]   Tanaka AJ, Bai R, Cho MT, Anyane-Yeboa K, Ahimaz P, Wilson AL, et al. De novo mutations in PURA are associated with hypotonia and developmental delay. Mol Case Stud 2015;1:a000356. doi:10.1101/mcs.a000356.

[29]   Reijnders MRF, Janowski R, Alvi M, Self JE, van Essen TJ, Vreeburg M, et al. PURA syndrome: clinical delineation and genotype-phenotype study in 32 individuals with review of published literature. J Med Genet 2017:jmedgenet-2017-104946. doi:10.1136/jmedgenet-2017-104946.

[30]   Johannesen KM, Gardella E, Gjerulfsen CE, Bayat A, Rouhl RPW, Reijnders M, et al. PURA-Related Developmental and Epileptic Encephalopathy: Phenotypic and Genotypic Spectrum. Neurol Genet 2021;7. doi:10.1212/NXG.0000000000000613.

[31]   Eldomery MK, Coban-Akdemir Z, Harel T, Rosenfeld JA, Gambin T, Stray-Pedersen A, et al. Lessons learned from additional research analyses of unsolved clinical exome cases. Genome Med 2017;9:1–15. doi:10.1186/s13073-017-0412-6.

[32]   Trau SP, Pizoli CE. PURA Syndrome and Myotonia. Pediatr Neurol 2020;104:62–3. doi:10.1016/J.PEDIATRNEUROL.2019.09.008.

[33]   Okamoto N, Nakao H, Niihori T, Aoki Y. Patient with a novel purine-rich element binding protein A mutation. Congenit Anom (Kyoto) 2017;57:201–4. doi:10.1111/cga.12214.

[34]   Mroczek M, Iyadurai S. Neuromuscular and Neuromuscular Junction Manifestations of the PURA-NDD: A Systematic Review of the Reported Symptoms and Potential Treatment Options. Int J Mol Sci 2023;24. doi:10.3390/ijms24032260.

[35]   Mayorga L, Gamboni B, Mampel A, Roqué M. A frame-shift deletion in the PURA gene associates with a new clinical finding: Hypoglycorrhachia. Is GLUT1 a new PURA target? Mol Genet Metab 2018. doi:10.1016/j.ymgme.2017.12.436.

[36]   Hokkanen S, Feldmann HM, Ding H, Jung CKE, Bojarski L, ller IRM, et al. Lack of pur-alpha alters postnatal brain development and causes megalencephaly. Hum Mol Genet 2012;21:473–84. doi:10.1093/hmg/ddr476.

[37]   Khalili K, Del Valle L, Muralidharan V, Gault WJ, Darbinian N, Otte J, et al. Purα Is Essential for Postnatal Brain Development and Developmentally Coupled Cellular Proliferation As Revealed by Genetic Inactivation in the Mouse. Mol Cell Biol 2003;23:6857–75.

doi:10.1128/mcb.23.19.6857-6875.2003.

[38] Koepsell H. Glucose transporters in brain in health and disease. Pflugers Arch Eur J Physiol 2020;472:1299–343. doi:10.1007/s00424-020-02441-x.

[39] Yu M, Sun N, Buajieerguli M, Xie Y, Meng H. Glucose Transporter Type 1 Deficiency Syndrome. Chinese J Neurol 2018;53:138–42. doi:10.3760/cma.j.issn.1006-7876.2020.02.012.

[40] Klepper J, Akman C, Armeno M, Auvin S, Cervenka M, Cross HJ, et al. Glut1 Deficiency Syndrome (Glut1DS): State of the art in 2020 and recommendations of the international Glut1DS study group. Epilepsia Open 2020;5:354–65. doi:10.1002/epi4.12414.

[41] Abraham MJ, Murtola T, Schulz R, Páll S, Smith JC, Hess B, et al. Gromacs: High performance molecular simulations through multi-level parallelism from laptops to supercomputers. SoftwareX 2015;1–2:19–25. doi:10.1016/j.softx.2015.06.001.

[42] Jo S, Kim T, Iyer VG, Im W. CHARMM-GUI: A web-based graphical user interface for CHARMM. J Comput Chem 2008;29:1859–65. doi:10.1002/JCC.20945.

[43] Berdasco M, Esteller M. Genetic syndromes caused by mutations in epigenetic genes. HumGenet 2013;132:359–83.

[44] Parrinello M, Rahman A. Polymorphic transitions in single crystals: A new molecular dynamics method. J Appl Phys 1981;52:7182–90. doi:10.1063/1.328693.

[45] SH. A molecular dynamics method for simulations in the canonical ensemble{. Mol Phys 2002;100. doi:10.1080/0026897011008910.

[46] Essmann U, Perera L, Berkowitz ML, Darden T, Lee H, Pedersen LG. A smooth particle mesh Ewald method. J Chem Phys 1995;103:8577–93.

[47] Hess B, Bekker H, C Berendsen HJ, E M Fraaije JG. 3 LINCS: a linear constraint solver for molecular simulations 1997;18:1463–72.

[48] Humphrey W, Dalke A, Schulten K. VMD: Visual molecular dynamics. J Mol Graph 1996;14:33–8. doi:10.1016/0263-7855(96)00018-5.

[49] Hamrahian AH, Zhang JZ, Elkhairi FS, Prasad R, Ismail-Beigi F. Activation of Glut1 glucose transporter in response to inhibition of oxidative phosphorylation. Role of sites of mitochondrial inhibition and mechanism of Glut1 activation. Arch Biochem Biophys 1999;368:375–9. doi:10.1006/abbi.1999.1320.

[50] Ebert BL, Firth JD, Ratcliffe PJ. Hypoxia and mitochondrial inhibitors regulate expression of glucose transporter-1 via distinct cis-acting sequences. J Biol Chem 1995;270:29083–9. doi:10.1074/jbc.270.49.29083.

[51] Jumper J, Evans R, Pritzel A, Green T, Figurnov M, Ronneberger O, et al. Highly accurate protein structure prediction with AlphaFold. Nature 2021;596:583–9. doi:10.1038/s41586-021-03819-2.

[52] Deng D, Xu C, Sun P, Wu J, Yan C, Hu M, et al. Crystal structure of the human glucose transporter GLUT1. Nature 2014;510:121–5. doi:10.1038/nature13306.

[53] Custódio TF, Paulsen PA, Frain KM, Pedersen BP. Structural comparison of GLUT1 to GLUT3 reveal transport regulation mechanism in sugar porter family. Life Sci Alliance 2021;4. doi:10.26508/LSA.202000858.

[54] Heather L. Wieman, Sarah R. Horn, Sarah R. Jacobs, , Brian J. Altman S, Kornbluth and JCR. An Essential Role for the Glut1 PDZ-Binding Motif in Growth Factor Regulation of Glut1 Degradation and Trafficking. Biochem J 2009;418:345–367.

[55] Chen R, Li L, Weng Z. ZDOCK: an initial-stage protein-docking algorithm. Proteins 2003;52:80–7. doi:10.1002/PROT.10389.

[56] Pierce BG, Wiehe K, Hwang H, Kim BH, Vreven T, Weng Z. ZDOCK server: interactive docking prediction of protein-protein complexes and symmetric multimers. Bioinformatics 2014;30:1771–3. doi:10.1093/BIOINFORMATICS/BTU097.

[57] May A, Zacharias M. Protein-ligand docking accounting for receptor side chain and global flexibility in normal modes: evaluation on kinase inhibitor cross docking. J Med Chem 2008;51:3499–506. doi:10.1021/JM800071V.

[58] Madadkar-Sobhani A, Guallar V. PELE web server: atomistic study of biomolecular systems at your fingertips. Nucleic Acids Res 2013;41. doi:10.1093/NAR/GKT454.

[59] Mintseris J, Pierce B, Wiehe K, Anderson R, Chen R, Weng Z. Integrating statistical pair potentials into protein complex prediction. Proteins 2007;69:511–20. doi:10.1002/PROT.21502.

[60] Lee J, Cheng X, Swails JM, Yeom MS, Eastman PK, Lemkul JA, et al. CHARMM-GUI Input Generator for NAMD, GROMACS, AMBER, OpenMM, and CHARMM/OpenMM Simulations Using the CHARMM36 Additive Force Field. J Chem Theory Comput 2016;12:405–13. doi:10.1021/acs.jctc.5b00935.

[61] Ruiz-Ciancio D, Lin LH, Veeramani S, Barros MN, Sanchez D, Di Bartolo AL, et al. Selection of a novel cell-internalizing RNA aptamer specific for CD22 antigen in B cell acute lymphoblastic leukemia. Mol Ther Nucleic Acids 2023;33:698–712. doi:10.1016/J.OMTN.2023.07.028.

[62] Masone D, Cabeza de Vaca I, Pons C, Recio JF, Guallar V. H-bond network optimization in protein-protein complexes: Are all-atom force field scores enough? Proteins Struct Funct Bioinforma 2012;80:818–24. doi:10.1002/prot.23239.

[63] Pei Y, Lv S, Shi Y, Jia J, Ma M, Han H, et al. RAB21 controls autophagy and cellular energy homeostasis by regulating retromer-mediated recycling of SLC2A1/GLUT1. Autophagy 2023;19:1070–86. doi:10.1080/15548627.2022.2114271.

[64] Bunn RC, Jensen MA, Reed BC. Protein interactions with the glucose transporter binding protein GLUT1CBP that provide a link between GLUT1 and the cytoskeleton. Mol Biol Cell 1999;10:819–32. doi:10.1091/mbc.10.4.819.

[65] Reed BC, Cefalu C, Bellaire BH, Cardelli JA, Louis T, Salamon J, et al. GLUT1CBP(TIP2/GIPC1) interactions with GLUT1 and myosin VI: evidence supporting an adapter function for GLUT1CBP. Mol Biol Cell 2005;16:4183–201. doi:10.1091/MBC.E04-11-0978.

[66] Mitsumori K, Takei Y, Hirokawa N. Components of RNA granules affect their localization and dynamics in neuronal dendrites. Mol Biol Cell 2017;28:1412–7. doi:10.1091/mbc.E16-07-

0497.

[67] Harris DS, Slot JW, Geuze HJ, James DE. Polarized distribution of glucose transporter isoforms in Caco-2 cells. Proc Natl Acad Sci U S A 1992;89:7556–60. doi:10.1073/pnas.89.16.7556.

[68] Cornford EM, Hyman S. Localization of brain endothelial luminal and abluminal transporters with immunogold electron microscopy. NeuroRx 2005;2:27–43. doi:10.1602/neurorx.2.1.27.

Supplementary material